PHYSICAL REVIEW E **93**, 051102(R) (2016)

Momentum and heat transport scalings in laminar vertical convection

Olga Shishkina*

Max Planck Institute for Dynamics and Self-Organization, Am Fassberg 17, D-37077 Göttingen, Germany

(Received 12 February 2016; published 23 May 2016)

We derive the dependence of the Reynolds number Re and the Nusselt number Nu on the Rayleigh number Ra and the Prandtl number Pr in laminar vertical convection (VC), where a fluid is confined between two differently heated isothermal vertical walls. The boundary layer equations in laminar VC yield two limiting scaling regimes: $\mathrm{Nu} \sim \mathrm{Pr}^{1/4}\,\mathrm{Ra}^{1/4}, \mathrm{Re} \sim \mathrm{Pr}^{-1/2}\,\mathrm{Ra}^{1/2}$ for $\mathrm{Pr} \ll 1$ and $\mathrm{Nu} \sim \mathrm{Pr}^{0}\,\mathrm{Ra}^{1/4}, \mathrm{Re} \sim \mathrm{Pr}^{-1}\,\mathrm{Ra}^{1/2}$ for $\mathrm{Pr} \gg 1$. These theoretical results are in excellent agreement with direct numerical simulations for Ra from 10^5 to 10^{10} and Pr from 10^{-2} to 30. The transition between the regimes takes place for Pr around 10^{-1}.

DOI: 10.1103/PhysRevE.93.051102

Thermally driven flows are ubiquitous in nature. The classically paradigmatic systems for studying such flows are Rayleigh-Bénard convection (RBC) [1–7], where a fluid is confined between a heated bottom plate and a cooled top plate, horizontal convection (HC) [8–10], where the fluid is heated at one part of the bottom plate and cooled at some other part, and vertical convection (VC), where the fluid is confined between two differently heated isothermal vertical walls [11–13]. The different boundary conditions (BCs) and convection cell geometries are known to significantly influence the mean convective heat and momentum transport [14–17], measured by the Nusselt number (Nu) and Reynolds number (Re), respectively.

In VC, as in RBC, the mean characteristics of the flow are determined by the Rayleigh number $\mathrm{Ra} \equiv \alpha g \Delta H^3/(\kappa\nu)$, the Prandtl number $\mathrm{Pr} \equiv \nu/\kappa$, and the cell geometry. Here, ν denotes the kinematic viscosity, κ the thermal diffusivity, α the isobaric thermal expansion coefficient of the fluid, g the acceleration due to gravity, H the diameter of the plates (in VC) or distance between the plates (in RBC), and $\Delta \equiv T_+ - T_- > 0$, with T_+ and T_- the temperature of, respectively, the heated and cooled plates.

How Re and Nu scale with Ra and Pr is one of the main issues in the study of thermally driven flows. For RBC, where the time- and volume-averaged kinetic dissipation rate (ϵ_u) and thermal dissipation rate (ϵ_θ) are exactly expressed in terms of Ra, Nu, and fluid properties, Grossmann and Lohse developed a scaling theory (GL) [18,19], which is based on a decomposition of ϵ_u and ϵ_θ into their boundary-layer (BL) and bulk contributions and their further analysis. The theory successfully predicts heat transport in RBC [1,20] and is also applicable to HC [10]. In contrast to RBC, in VC, the exact relation for ϵ_u generally does not hold, which impedes the applicability of GL to predict the scalings in VC.

Previous experimental and numerical studies of VC report the scaling exponent β in the power law $\mathrm{Nu} \sim \mathrm{Ra}^\beta$, varying from 1/4 to 1/3. In laminar VC it is about 1/4 [21–24], being slightly larger for very small Ra, where the geometrical cell confinement influences the heat transport [11,13,25,26], and for very large Ra, where the VC flows become fully turbulent [27,28]. The dependences of Nu on Pr and of Re on Ra and Pr in VC have been less investigated. For similar cell geometry and ranges of Ra and Pr, the heat transport in VC (from vertical surfaces) generally differs from that in RBC (from horizontal surfaces) [11,29–33]. Furthermore, for the same Ra, Pr, and cell geometry, the VC and RBC flows can be in different states. For example, for $\mathrm{Pr} = 1$, $\mathrm{Ra} = 10^8$, and a cylindrical container of aspect ratio 1, the VC flow is steady, while the RBC flow is turbulent, as has been shown in direct numerical simulations (DNS), where the inclination angle of the cell varied from 0 (RBC) to $\pi/2$ (VC) [12].

In this Rapid Communication we derive the dependences of Re and Nu on Ra and Pr in laminar VC, based on an analysis of the BL equations. The theoretical scalings of Nu and Re with Ra are supported by the DNS of VC in a cylindrical container of equal height and diameter, for $\mathrm{Pr} = 0.1$, 1, and 10 in the range $10^5 \leqslant \mathrm{Ra} \leqslant 10^{10}$, while the scalings of Nu and Re with Pr are supported by the DNS for $\mathrm{Ra} = 10^6$ and 10^7 in the range $10^{-2} \leqslant \mathrm{Pr} \leqslant 30$ (Fig. 1). We show that the theoretical predictions are in excellent agreement with the DNS results (Fig. 3).

Following Ostrach [34], we consider a fluid flow along a vertical heated plate and set up the coordinate system so that the x direction is along the plate and the z direction is horizontal away from the plate. We assume that the mean flow in the other horizontal direction is much weaker than that in x or z and, therefore, consider a two-dimensional flow that depends on x and z only. Under the standard BL approximation we obtain the BL equations (1)–(3) with BCs (4) and (5) for fluid motion near a hot vertical plate,

$$u_x \partial_x u_x + u_z \partial_z u_x = \nu \partial_z^2 u_x + \alpha g (T - T_0), \tag{1}$$

$$u_x \partial_x T + u_z \partial_z T = \kappa \partial_z^2 T, \tag{2}$$

$$\partial_x u_x + \partial_z u_z = 0, \tag{3}$$

$$u_x(x,0) = u_z(x,0) = 0, \quad T(x,0) = T_+, \tag{4}$$

$$u_x(x,\infty) = 0, \quad T(x,\infty) = T_0, \tag{5}$$

where (u_x, u_z) is the velocity vector in the coordinates (x,z) and T denotes the temperature, $T_0 = (T_+ + T_-)/2$.

Note that in the case when the heated plate is placed horizontally, as in RBC, the last term in (1) is absent, since the buoyancy is orthogonal to the plate, and in the BCs

*Olga.Shishkina@ds.mpg.de

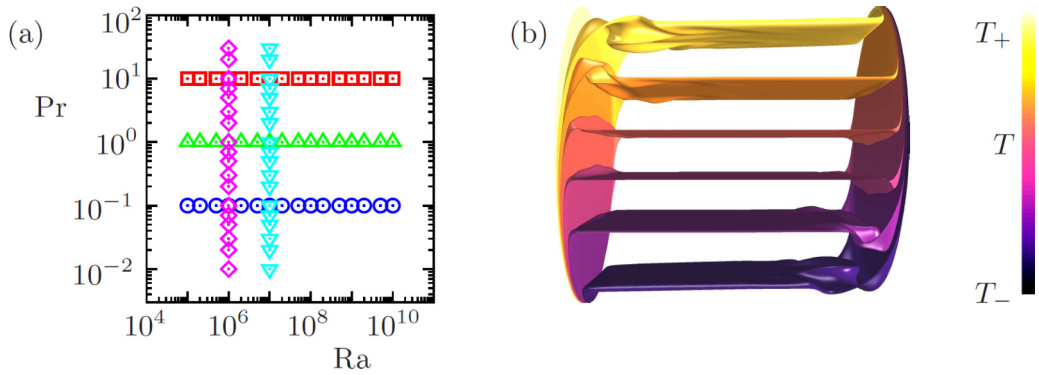

FIG. 1. (a) Sketch of the conducted DNS of VC in a cylindrical cell filled with a fluid of Pr = 0.1 (dotted circle), Pr = 1 (upward triangle), Pr = 10 (dotted square), and Ra = 10^6 (dotted diamond), Ra = 10^7 (downward triangle), in a (Ra,Pr) plane. (b) Eight isosufaces of the instantaneous temperature T, as obtained in the DNS for Pr = 1 and Ra = 10^8. The left vertical wall of the container is heated ($T = T_+$), while the right vertical wall is cooled ($T = T_-$); the other walls are adiabatic.

$u_x(x,\infty) = U \neq 0$ is assumed, where U is the flow velocity above the plate, i.e., the so-called wind outside the BL. The resulting BL momentum equation (1) without a buoyancy term was first derived by Prandtl [35,36] and solved by Blasius [37] for a constant flow above an infinite horizontal plate, while Eq. (2) was obtained first by Pohlhausen [38]. For a generalization of this approach to a nonconstant wind above the horizontal plate (or to a nonvanishing pressure gradient within the BL), we refer to Refs. [39,40], and for a generalization due to the influence of the fluctuations within the BL, we refer to Ref. [6].

In the case of a vertical heated plate, as in VC, a buoyancy term is present in (1). Considering a similarity variable $\eta \propto z\,x^{-1/4}$ and stream function $\Psi \propto x^{3/4}F(\eta)$, Ostrach [34] showed that for a similarity solution to exist, Nu must scale as $\sim \mathrm{Ra}^{1/4}$, where the proportionality coefficient depends on Pr and $F(\eta)$ is a function of η. Numerical solutions [34] of the resulting BL equations for particular Pr were found to be in good agreement with measurements of Nu at the vertical hot plate for laminar flows in air [21], oil [22], and mercury [23].

Below we advance the approach [34] in such a way that it allows us to find the Nu and Re scalings with respect to Ra and Pr in laminar VC. The idea of the method is the following. Let us consider the similarity variable ξ, stream function Ψ, and temperature T in the forms

$$\xi = \mathrm{Pr}^a\,\mathrm{Ra}^b (z/H)(x/H)^c, \tag{6}$$

$$\Psi = \mathrm{Pr}^d\,\mathrm{Ra}^e\,\nu(x/H)^f\phi(\xi), \quad u_x = \partial_z\Psi, \quad u_z = -\partial_x\Psi, \tag{7}$$

$$T = T_0 + (T_+ - T_0)\theta(\xi) = T_0 + (\Delta/2)\theta(\xi). \tag{8}$$

If there exist certain constants a, b, c, d, e, and f such that the resulting BL equations for VC depend exclusively on ξ, $\phi(\xi)$, and $\theta(\xi)$, and do not depend explicitly on Pr and Ra (as well as their BCs), then $\theta_\xi(0)$ is independent of Ra and Pr. (Here the subscript ξ denotes the derivative with respect to ξ.) In this case, the Nusselt number

$$\mathrm{Nu} \equiv \frac{-H^{-1}\int_0^H \kappa\,\partial_z T|_{z=0}\,dx}{\kappa\Delta/H} = \frac{-\theta_\xi(0)}{2(c+1)}\mathrm{Pr}^a\,\mathrm{Ra}^b, \tag{9}$$

scales as $\sim \mathrm{Pr}^a\,\mathrm{Ra}^b$. Analogously one can derive the scaling of the Reynolds number, which is defined on the maximal mean velocity along the heated plate, i.e.,

$$\mathrm{Re} \equiv UH/\nu, \quad U \equiv \max_z H^{-1}\int_0^H u_x\,dx. \tag{10}$$

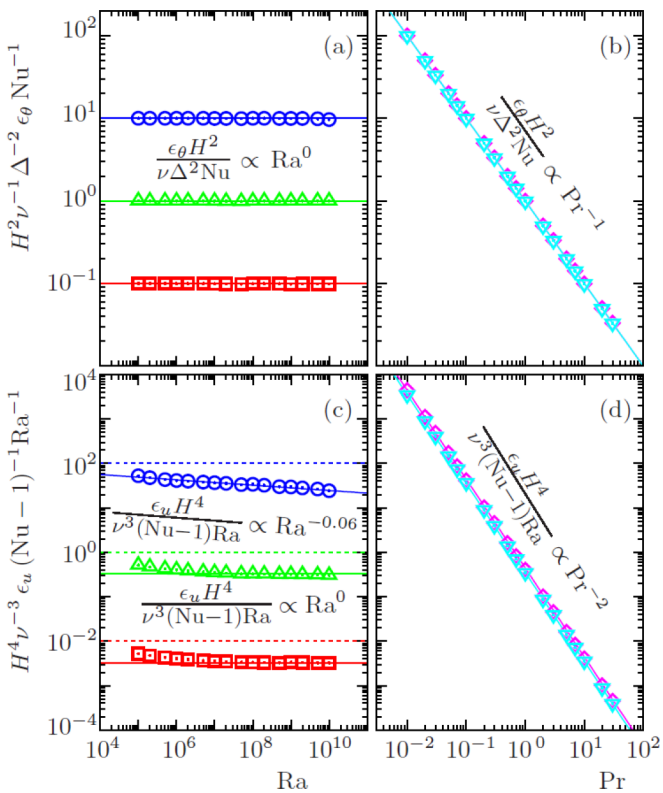

FIG. 2. (a), (c) Ra dependences and (b), (d) Pr dependences of (a), (b) the mean thermal dissipation rate ϵ_θ and (c), (d) the mean kinetic dissipation rate ϵ_u, as obtained in the DNS of VC for (a), (c) Pr = 0.1 (dotted circle), Pr = 1 (upward triangle), Pr = 10 (dotted square), and for (b), (d) Ra = 10^6 (dotted diamond) and Ra = 10^7 (downward triangle). Dashed lines in (c) show the corresponding exact values for RBC.

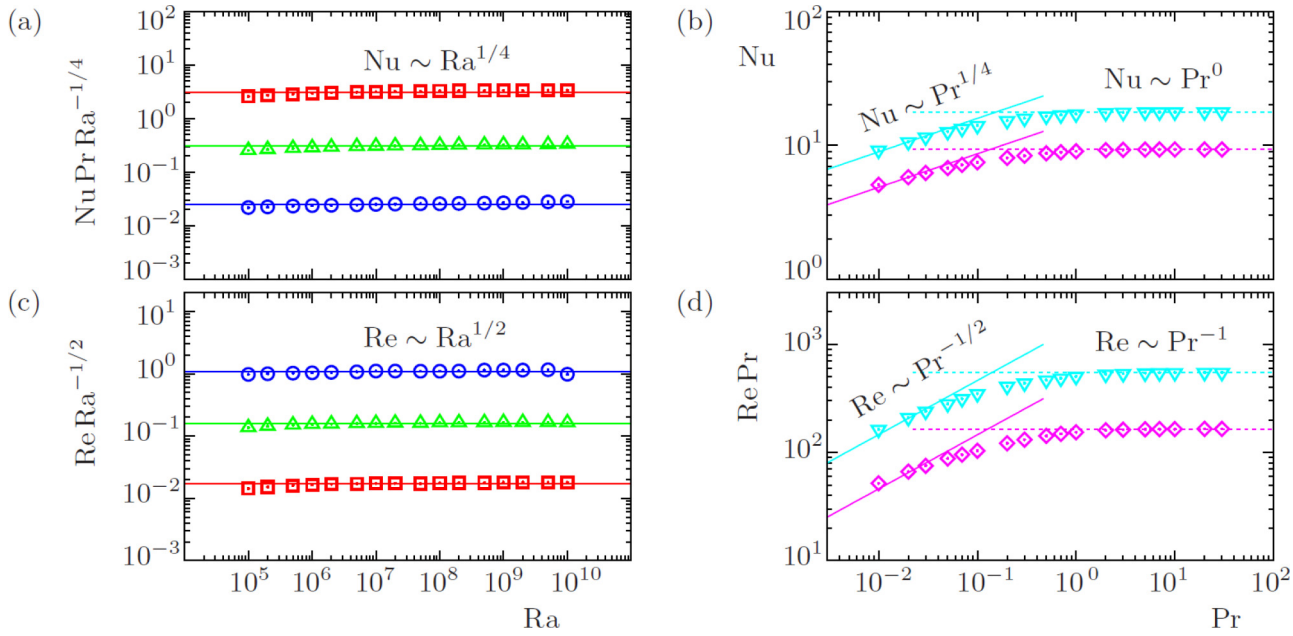

FIG. 3. (a), (c) Ra dependences and (b), (d) Pr dependences of (a), (b) the Nusselt number and (c), (d) the Reynolds number, as obtained in the DNS of VC for (a), (c) Pr = 0.1 (dotted circle), Pr = 1 (upward triangle), Pr = 10 (dotted square), and for (b), (d) Ra = 10^6 (dotted diamond) and Ra = 10^7 (downward triangle). For laminar vertical convection the simulations support the scalings Nu $\sim$ $\mathrm{Pr}^{1/4}\,\mathrm{Ra}^{1/4}$, Re $\sim$ $\mathrm{Pr}^{-1/2}\,\mathrm{Ra}^{1/2}$ for small Pr [Eq. (22)], and Nu $\sim$ $\mathrm{Pr}^{0}\,\mathrm{Ra}^{1/4}$, Re $\sim$ $\mathrm{Pr}^{-1}\,\mathrm{Ra}^{1/2}$ for large Pr [Eq. (20)]. There is a transition from one scaling regime to another at Pr $\approx$ 0.1.

Indeed, the vertical velocity equals

$$u_x = \partial_z \Psi = \mathrm{Pr}^{a+d}\,\mathrm{Ra}^{b+e}(\nu/H)(x/H)^{c+f}\phi_\xi \qquad (11)$$

and its maximum is achieved at a certain value of $\xi = \hat{\xi}$, where $\phi_{\xi\xi}(\hat{\xi}) = 0$. From (10) and (11) we obtain

$$\mathrm{Re} = \mathrm{Pr}^{a+d}\,\mathrm{Ra}^{b+e}(c+f+1)^{-1}\phi_\xi\big(\hat{\xi}\big). \qquad (12)$$

Thus, Re $\sim$ $\mathrm{Pr}^{a+d}\,\mathrm{Ra}^{b+e}$ if there exist constants a, b, c, d, e, and f such that the BL equations for $\phi(\xi)$ (7) and $\theta(\xi)$ (8) and their BCs are independent of Pr and Ra.

From (4) and (5) and (6)–(8) we obtain that the BCs for ϕ and θ are indeed independent of Pr and Ra, i.e., $\phi(0) = \phi_\xi(0) = 0$, $\phi_\xi(\infty) = 0$, and $\theta(0) = 1$, $\theta(\infty) = 0$. To find the desired constants a, b, c, d, e, and f, we substitute (6)–(8) into (1) and (2) and require the independence of the resulting BL equations from Pr and Ra. Thus, the substitution into the energy equation (2) leads to

$$\theta_{\xi\xi} + f\,\mathrm{Pr}^{d-a+1}\,\mathrm{Ra}^{e-b}(x/H)^{f-c-1}\phi\,\theta_\xi = 0, \qquad (13)$$

and, hence, the constants are related as follows:

$$d = a - 1, \quad e = b, \quad f = c + 1. \qquad (14)$$

The energy equation (13) is then reduced to

$$\theta_{\xi\xi} + (c+1)\phi\,\theta_\xi = 0. \qquad (15)$$

Using (6)–(8) and (14), from (1) we obtain

$$\mathrm{Pr}^{4a}\,\phi_{\xi\xi\xi} + \mathrm{Pr}^{4a-1}[(c+1)\phi\phi_{\xi\xi} - (2c+1)(\phi_\xi)^2] - \mathrm{Ra}^{1-4b}(x/H)^{-4c-1}\theta/2 = 0. \qquad (16)$$

For the independence of the momentum equation (16) from Ra and for the existence of the similarity solution with respect to ξ, the constants b and c must be equal to

$$b = 1/4, \quad c = -1/4, \qquad (17)$$

and, therefore, (16) is reduced to

$$4\,\mathrm{Pr}^{4a}\,\phi_{\xi\xi\xi} + \mathrm{Pr}^{4a-1}[3\phi\phi_{\xi\xi} - 2(\phi_\xi)^2] - 2\theta = 0. \qquad (18)$$

For Pr $\gg$ 1 the first term in (18) dominates the second one, therefore a must be taken equal to 0 and the second term in (18) is negligible in this case. Thus, for Pr $\gg$ 1,

$$a = 0, \quad b = \tfrac{1}{4}, \quad c = -\tfrac{1}{4}, \quad d = -1, \quad e = \tfrac{1}{4}, \quad f = \tfrac{3}{4}, \qquad (19)$$

and Nu (9) and Re (12) scale with Pr and Ra as

$$\mathrm{Nu} \sim \mathrm{Pr}^{0}\,\mathrm{Ra}^{1/4},\ \mathrm{Re} \sim \mathrm{Pr}^{-1}\,\mathrm{Ra}^{1/2},\ \text{for Pr} \gg 1. \qquad (20)$$

For Pr $\ll$ 1, the first term in (18) is negligible and $a = 1/4$. In this case,

$$a = \tfrac{1}{4}, \quad b = \tfrac{1}{4}, \quad c = -\tfrac{1}{4}, \quad d = -\tfrac{3}{4}, \quad e = \tfrac{1}{4}, \quad f = \tfrac{3}{4}, \qquad (21)$$

and the corresponding scalings are

$$\mathrm{Nu} \sim \mathrm{Pr}^{1/4}\,\mathrm{Ra}^{1/4},\ \mathrm{Re} \sim \mathrm{Pr}^{-1/2}\,\mathrm{Ra}^{1/2},\ \text{for Pr} \ll 1. \qquad (22)$$

To check whether the scalings (20) and (22) hold in laminar VC for, respectively, large and small Pr, a set of simulations was conducted (Fig. 1). The code used was GOLDFISH, as in Refs. [6,12], and the mesh resolution requirements of Ref. [41] were fulfilled. The number of computational grid nodes ranges from 2.4×10^6 for Ra = 10^5 to 1.5×10^8 for Ra = 10^{10}, which correspond to the grids $96 \times 128 \times 192$ and $384 \times 512 \times 768$ in cylindrical coordinates (r,φ,z), respectively.

In VC, as in RBC, the exact relation $H^2/(\kappa\Delta^2)\,\epsilon_\theta = \mathrm{Nu}$ always holds [Figs. 2(a) and 2(b)]. In contrast, the values of $(H^4/\nu^3)(\mathrm{Nu}-1)^{-1}\,\mathrm{Ra}^{-1}\epsilon_u$ are always smaller than the corresponding values in RBC (i.e., Pr^{-2}) [Fig. 2(c)]. For small Pr, this quantity gradually decreases as $\sim\mathrm{Ra}^{-0.06}$ with growing Ra [Fig. 2(c)], although its proportionality to Pr^{-2} still holds [Fig. 2(d)].

The here derived scalings (20) and (22) are fully supported by the simulations, as one can see in Fig. 3. In all studied cases $\mathrm{Nu} \sim \mathrm{Ra}^{1/4}$ [Fig. 3(a)] and $\mathrm{Re} \sim \mathrm{Ra}^{1/2}$ [Fig. 3(c)]. A slightly faster growth of Nu with Ra is obtained for $\mathrm{Ra} \leqslant 10^6$, where the geometrical confinement of the convection cell influences the heat and mass transport. A similar increase of the scaling exponent for small Ra was found also in Refs. [11,13,25,26]. For small Pr the heat flux scales with Pr as $\mathrm{Nu} \sim \mathrm{Pr}^{1/4}$, while for large Pr the Nusselt number is independent of Pr [Fig. 3(b)]. The Reynolds number scales as $\mathrm{Re} \sim \mathrm{Pr}^{-1/2}$ for small Pr and as $\mathrm{Re} \sim \mathrm{Pr}^{-1}$ for large Pr [Fig. 3(d)]. The transition from one regime to another takes place for Pr on the order of 10^{-1}.

In summary, a slight advancement of the Prandtl approach [35] to study laminar BLs allowed us to derive the scalings of Nu and Re with Ra and Pr in laminar VC. The simulation results for VC in a cylindrical convection cell with equal height and diameter, for Ra from 10^5 to 10^{10} and Pr from 10^{-2} to 30, are in excellent agreement with the theoretical predictions.

O.S. thanks Eberhard Bodenschatz, Susanne Horn, and Detlef Lohse for fruitful discussions and acknowledges the financial support of the Deutsche Forschungsgemeinschaft (DFG) under Grant No. Sh405/4–Heisenberg fellowship and the Leibniz Supercomputing Centre (LRZ) for providing computing time.

[1] G. Ahlers, S. Grossmann, and D. Lohse, Rev. Mod. Phys. **81**, 503 (2009).
[2] E. Bodenschatz, W. Pesch, and G. Ahlers, Annu. Rev. Fluid Mech. **32**, 709 (2000).
[3] F. Chillà and J. Schumacher, Eur. Phys. J. E **35**, 58 (2012).
[4] E. Siggia, Annu. Rev. Fluid Mech. **26**, 137 (1994).
[5] C. R. Doering, F. Otto, and M. G. Reznikoff, J. Fluid Mech. **560**, 229 (2006).
[6] O. Shishkina, S. Horn, S. Wagner, and E. S. C. Ching, Phys. Rev. Lett. **114**, 114302 (2015).
[7] X. He, E. S. C. Ching, and P. Tong, Phys. Fluids **23**, 025106 (2011).
[8] G. O. Hughes and R. W. Griffiths, Annu. Rev. Fluid Mech. **40**, 185 (2008).
[9] O. Shishkina and S. Wagner, Phys. Rev. Lett. **116**, 024302 (2016).
[10] O. Shishkina, S. Grossmann, and D. Lohse, Geophys. Res. Lett. **43**, 1219 (2016).
[11] C. S. Ng, A. Ooi, D. Lohse, and D. Chung, J. Fluid Mech. **764**, 349 (2015).
[12] O. Shishkina and S. Horn, J. Fluid Mech. **790**, R3 (2016).
[13] H. Yu, N. Li, and R. E. Ecke, Phys. Rev. E **76**, 026303 (2007).
[14] P. Hassanzadeh, G. P. Chini, and C. R. Doering, J. Fluid Mech. **751**, 627 (2014).
[15] M. Gibert, H. Pabiou, F. Chillà, and B. Castaing, Phys. Rev. Lett. **96**, 084501 (2006).
[16] Z. A. Daya and R. E. Ecke, Phys. Rev. Lett. **87**, 184501 (2001).
[17] G. Boffetta and R. E. Ecke, Annu. Rev. Fluid Mech. **44**, 427 (2012).
[18] S. Grossmann and D. Lohse, J. Fluid Mech. **407**, 27 (2000).
[19] S. Grossmann and D. Lohse, Phys. Rev. Lett. **86**, 3316 (2001).
[20] R. J. A. M. Stevens, E. P. van der Poel, S. Grossmann, and D. Lohse, J. Fluid Mech. **730**, 295 (2013).
[21] E. Schmidt and W. Beckmann, Forsch. Ingenieurwes. (Techn. Mech. Thermodyn.) **1**, 341 (1930).
[22] H. H. Lorenz, Z. Tech. Phys. **9**, 362 (1934).
[23] O. A. Saunders, Proc. R. Soc. London, Ser. A **172**, 55 (1939).
[24] S. W. Churchill and H. H. S. Chu, Int. J. Heat Mass Transfer **18**, 1323 (1975).
[25] T. A. M. Versteegh and F. T. M. Nieuwstadt, Int. J. Heat Mass Transfer **42**, 3673 (1999).
[26] P. Kis and H. Herwig, Int. J. Heat Mass Transfer **55**, 2625 (2012).
[27] W. K. George and S. P. Capp, Int. J. Heat Mass Transfer **22**, 813 (1979).
[28] T. Fujii, M. Takeuchi, M. Fujii, K. Suzaki, and H. Uehar, Int. J. Heat Mass Transfer **13**, 753 (1970).
[29] J. Bailon-Cuba, O. Shishkina, C. Wagner, and J. Schumacher, Phys. Fluids **24**, 107101 (2012).
[30] O. Shishkina and C. Wagner, J. Fluid Mech. **686**, 568 (2011).
[31] O. Shishkina and C. Wagner, J. Turbulence **13**, 1 (2012).
[32] S. Wagner and O. Shishkina, Phys. Fluids **25**, 085110 (2013).
[33] S. Wagner and O. Shishkina, J. Fluid Mech. **763**, 109 (2015).
[34] S. Ostrach, NACA Rep. **1111**, 63 (1953).
[35] L. Prandtl, in *Verhandlungen des III. Int. Math. Kongr., Heidelberg, 1904* (Teubner, Leipzig, 1905), pp. 484–491.
[36] L. D. Landau and E. M. Lifshitz, *Fluid Mechanics*, 2nd ed., Course of Theoretical Physics Vol. 6 (Butterworth-Heinemann, Oxford, UK, 1987).
[37] H. Blasius, Z. Math. Phys. **56**, 1 (1908).
[38] E. Pohlhausen, Z. Angew. Math. Mech. **1**, 115 (1921).
[39] O. Shishkina, S. Horn, and S. Wagner, J. Fluid Mech. **730**, 442 (2013).
[40] O. Shishkina, S. Wagner, and S. Horn, Phys. Rev. E **89**, 033014 (2014).
[41] O. Shishkina, R. J. A. M. Stevens, S. Grossmann, and D. Lohse, New J. Phys. **12**, 075022 (2010).